Subdomain Perturbation Finite Element Method for Skin and Proximity Effects in Inductors

Patrick Dular, Ruth V. Sabariego and Laurent Krähenbühl

Purpose – To develop a subdomain perturbation technique to calculate skin and proximity effects in inductors within frequency and time domain finite element (FE) analyses.

Design/methodology/approach – A reference limit eddy current FE problem is first solved by considering perfect conductors via appropriate boundary conditions. Its solution gives the source for eddy current FE perturbation subproblems in each conductor with its actual conductivity. Each of these problems requires an appropriate mesh of the associated conductor and its surrounding region.

Findings – The skin and proximity effects in inductors can be accurately determined in a wide frequency range, allowing for a precise consideration of inductive phenomena as well as Joule losses calculations in thermal coupling.

Originality/value – The developed subdomain method allows to accurately determine the current density distributions and ensuing Joule losses in conductors of any shape, not only in the frequency domain but also in the time domain. It extends the domain of validity and applicability of impedance boundary condition techniques. It also allows the solution process to be lightened, as well as efficient parameterized analyses on signal forms and conductor characteristics.

Keywords – Impedance boundary condition, Perturbation technique, Subdomain finite element method, Skin and proximity effects, Time and frequency domains

Paper type – Research paper

I. Introduction

A precise consideration of the skin and proximity effects in conductors is important for an accurate calculation of their field distribution and the ensuing Joule losses. Calculating these effects with the classical finite element (FE) method usually presents difficulties. The mesh must be fine enough with respect to the skin depth in all the materials, which then leads to a large system of equations.

Impedance boundary conditions (IBCs) (Krähenbühl and Muller, 1993) defined on the conductor boundaries are an alternative to avoid meshing the conductor interior. Such boundary conditions (BCs) are nevertheless generally based on analytical solutions and in practice only valid far from any geometrical discontinuities, e.g. edges and corners. They are also generally restricted to frequency domain and linear analyses.

In this contribution, a method is developed to overcome the limitations of IBCs, considering conductors of any shape not only in the frequency domain but also in the time domain. The magnetic vector potential FE magnetodynamic formulation is used. The developed method is based on the coupling of reference and perturbation solutions (Badics *et al.*, 1997; Dular and Sabariego, 2007; Dular *et al.*, 2007), each of these being calculated in distinct meshes. A reference limit eddy current FE problem is first solved by considering perfect conductive properties, via appropriate BCs on the conductor boundaries. The solution of the limit problem gives the sources for FE perturbation subproblems in each conductor then considered with a finite conductivity. Each of these problems requires an appropriate volume mesh of the associated conductor and its surrounding region. The developed technique is validated on application examples. Its main advantages versus the IBC technique are pointed out.

This work was partly supported by the Belgian Science Policy (IAP P6/21) and the Belgian French Community (Research Concerted Action ARC 03/08-298).

P. Dular and R. V. Sabariego are with the University of Liège, Dept. of Electrical Engineering and Computer Science, B28, B-4000 Liège, Belgium (e-mail's: Patrick.Dular@ulg.ac.be, r.sabariego@ulg.ac.be). P. Dular is also with the Belgian Fund for Scientific Research (F.N.R.S.). L. Krähenbühl is with the Université de Lyon, F-69003 Lyon, France; he is also with the Laboratoire Ampère, UMR CNRS 5005, École Centrale de Lyon, F-69134 Écully Cedex, France (e-mail: Laurent.Krahenbuhl@ec-lyon.fr).

II. Reference and modified eddy current problems

A. Canonical problem in a strong form

A canonical problem p consists in solving the magnetodynamic equations in a bounded domain Ω_p, with boundary $\Gamma_p = \Gamma_{h,p} \cup \Gamma_{b,p} = \partial\Omega_p$ (possibly at infinity), of the 2-D or 3-D Euclidean space. The eddy current conducting part of Ω_p is denoted $\Omega_{c,p}$ and the non-conducting one $\Omega_{c,p}{}^C$, with $\Omega_p = \Omega_{c,p} \cup \Omega_{c,p}{}^C$. Massive conductors belong to $\Omega_{c,p}$. The subscript p of each object refers to the associated problem p.

The equations, material relations, boundary conditions (BCs) and interface conditions (ICs) of problem p are

$$\operatorname{curl} \boldsymbol{h}_p = \boldsymbol{j}_p\,, \quad \operatorname{curl} \boldsymbol{e}_p = -\partial_t \boldsymbol{b}_p\,, \quad \operatorname{div} \boldsymbol{b}_p = 0\,, \qquad \text{(1a-b-c)}$$

$$\boldsymbol{b}_p = \mu_p \boldsymbol{h}_p + \boldsymbol{b}_{s,p}\,, \quad \boldsymbol{j}_p = \sigma_p \boldsymbol{e}_p + \boldsymbol{j}_{s,p}\,, \qquad \text{(1d-e)}$$

$$\boldsymbol{n} \times \boldsymbol{h}_p|_{\Gamma_{h,p}} = 0\,, \quad \boldsymbol{n} \times \boldsymbol{e}_p|_{\Gamma_{e,p} \subset \Gamma_{b,p}} = 0\,, \quad \boldsymbol{n} \cdot \boldsymbol{b}_p|_{\Gamma_{b,p}} = 0\,, \qquad \text{(1f-g-h)}$$

$$[\boldsymbol{n} \times \boldsymbol{h}_p]_{\gamma_p} = \boldsymbol{j}_{su,p}, \; [\boldsymbol{n} \times \boldsymbol{e}_p]_{\gamma_p} = \boldsymbol{k}_{su,p}, \; [\boldsymbol{n} \cdot \boldsymbol{b}_p]_{\gamma_p} = \boldsymbol{b}_{su,p}, \qquad \text{(1i-j-k)}$$

where $\boldsymbol{h}_p$ is the magnetic field, $\boldsymbol{b}_p$ is the magnetic flux density, $\boldsymbol{e}_p$ is the electric field, $\boldsymbol{j}_p$ is the electric current density (including source and eddy currents), μ_p is the magnetic permeability, σ_p is the electric conductivity and $\boldsymbol{n}$ is the external unit normal to a boundary. As will be shown, fields $\boldsymbol{b}_{s,p}$ and $\boldsymbol{j}_{s,p}$ are source fields that will serve for the coupling of different subproblems. Note that (1b) is only expressed in $\Omega_{c,p}$, whereas it is reduced to the form (1c) in $\Omega_{c,p}{}^C$. Also (1g) is more restrictive than (1h). The notation $[\cdot]_\gamma = \cdot|_{\gamma^+} - \cdot|_{\gamma^-}$ expresses the discontinuity of a quantity through any interface γ (with sides γ^+ and γ^-), which is allowed to be non-zero. The associated surface fields $\boldsymbol{j}_{su,p}$, $\boldsymbol{k}_{su,p}$ and $\boldsymbol{b}_{su,p}$ may be either

known or not, respectively for fixing constraints or post-processing results. Both uses will be tackled.

B. Reference and perturbation problems

The objective is solving successive problems, the superposition of which gives the solution of a complete problem. For the case of two subproblems, the complete solution is

$$\boldsymbol{h}=\boldsymbol{h}_1+\boldsymbol{h}_2\ ,\ \boldsymbol{b}=\boldsymbol{b}_1+\boldsymbol{b}_2\ ,\ \boldsymbol{j}=\boldsymbol{j}_1+\boldsymbol{j}_2\ ,\ \boldsymbol{e}=\boldsymbol{e}_1+\boldsymbol{e}_2\ ,$$
$$\boldsymbol{j}_{su}=\boldsymbol{j}_{su,1}+\boldsymbol{j}_{su,2}\ ,\ \boldsymbol{k}_{su}=\boldsymbol{k}_{su,1}+\boldsymbol{k}_{su,2}\ ,\ \boldsymbol{b}_{su}=\boldsymbol{b}_{su,1}+\boldsymbol{b}_{su,2}\ . \qquad (2)$$

As first step, a problem $p=1$ of form (1) is defined and called reference or source problem. Its source fields in (1d-e) are set to zero

$$\boldsymbol{b}_{s,1}=0\ ,\quad \boldsymbol{j}_{s,1}=0\ . \qquad (3a\text{-}b)$$

Both small and large perturbations of this problem are considered. These can result from the change of properties of existing materials (Badics *et al.*, 1997) or from the addition of new materials in the ambient region (Dular and Sabariego, 2007), which actually also amounts to changing some material properties. A problem $p=2$ of same form (1) is then defined as a perturbation problem that results from a change of permeability or conductivity, from μ_1 to μ_2 or σ_1 to σ_2, in some subregions. It is defined in domain Ω_2, i.e. a modified form of Ω_1. For linear materials, the complete problem resulting from this perturbation has a solution with form (2) under the condition that the source fields in (1d-e) are given by

$$\boldsymbol{b}_{s,2}=(\mu_2-\mu_1)\,\boldsymbol{h}_1\ ,\quad \boldsymbol{j}_{s,2}=(\sigma_2-\sigma_1)\,\boldsymbol{e}_1\ . \qquad (4\text{-}5)$$

This way the sum of all the equations and relations of (1) respectively for $p=1$ and 2 gives exactly these of the complete problem. Nonlinear analyses can be classically treated inside each problem, with possible inter-problem iterations.

The perturbation fields are still governed by the classical Maxwell equations (1a-b-c) whereas their associated material relations include now the additional volume sources (4) and (5). These sources usefully only occur in the modified regions.

Solving the perturbation problem $p=2$ instead of the complete one enables to avoid operations already performed in the reference problem $p=1$. At the discrete level, the meshes of both reference and perturbation problems can be significantly simplified, each problem asking for mesh refinement of different regions.

C. Possible approximation of the perturbation problem

As an approximation, domain Ω_2 can disregard some materials initially present in domain Ω_1, while these must exist in the considered complete problem. At the discrete level, this allows to reduce the meshing operations and the computational efforts in solving the perturbation problem. In particular, any intersection of non-material regions of Ω_2 with the material regions of Ω_1 is thus allowed (Dular and Sabariego, 2007; Dular *et al.*, 2007).

With such an approximation, the sources (4) and (5) are not applied in the omitted material regions. The material relations for the complete fields in these regions are thus

$$\boldsymbol{b}_1+\boldsymbol{b}_2=\mu_1\,\boldsymbol{h}_1+\mu_2\,\boldsymbol{h}_2\ ,\quad \boldsymbol{j}_1+\boldsymbol{j}_2=\sigma_1\,\boldsymbol{e}_1+\sigma_2\,\boldsymbol{e}_2\ . \qquad (6a\text{-}b)$$

They can be transformed, with (2), as

$$\boldsymbol{b}=\mu_1\,\boldsymbol{h}+(\mu_2-\mu_1)\,\boldsymbol{h}_2\ ,\quad \boldsymbol{j}=\sigma_1\,\boldsymbol{e}+(\sigma_2-\sigma_1)\,\boldsymbol{e}_2\ , \qquad (7a\text{-}b)$$

to point out the error made when their second terms are not negligible. This is the case when the material properties differ too much between states 1 and 2, and the perturbation fields are too large compared to the reference fields. The correct relations, $\boldsymbol{b}=\mu_1\,\boldsymbol{h}$ and $\boldsymbol{j}=\sigma_1\,\boldsymbol{e}$, are only rigorously fulfilled in the regions where μ and σ are unchanged.

For large perturbations, iterations between these problems are required to ensure an accurate solution. Successive perturbations are thus to be calculated, not only from problem 1 to problem 2 but also from the latter to the former. The perturbation of problem 2 then becomes a source for problem 1 with, similarly to (4-5), the non-zero source fields

$$\boldsymbol{b}_{s,1}=(\mu_1-\mu_2)\,\boldsymbol{h}_2\ ,\quad \boldsymbol{j}_{s,1}=(\sigma_1-\sigma_2)\,\boldsymbol{e}_2\ . \qquad (8\text{-}9)$$

III. A REFERENCE PROBLEM WITH PERFECT CONDUCTORS

Some conductors $\Omega_{cpe,1}\subset\Omega_{c,1}\subset\Omega_1$, of boundary $\Gamma_{cpe,1}=\partial\Omega_{cpe,1}$, are first considered as perfect in the reference problem $p=1$. Their conductivity thus tends to infinity, which results in a zero limit skin depth and surface currents. The surface currents are considered to flow between the two ideal layers of $\Gamma_{cpe,1}$, denoted $\Gamma_{cpe,1}{}^{+}$ and $\Gamma_{cpe,1}{}^{-}$ (inner and outer sides with regard to $\Omega_{cpe,1}$). The domain $\Omega_{cpe,1}$ can be extracted from Ω_1 in (1) and treated via a BC of zero normal magnetic flux density on its boundary $\Gamma_{cpe,1}{}^{+}$. Given that no field exists in $\Omega_{cpe,1}$, the same BC appears on $\Gamma_{cpe,1}{}^{-}$. One thus has

$$\boldsymbol{n}\cdot\boldsymbol{b}_1|_{\Gamma_{cpe,1}{}^{+}}=0\ ,\quad \boldsymbol{n}\cdot\boldsymbol{b}_1|_{\Gamma_{cpe,1}{}^{-}}=0\ . \qquad (10a\text{-}b)$$

However, the trace of the magnetic field is unknown on $\Gamma_{cpe,1}{}^{+}$ and vanishes also on $\Gamma_{cpe,1}{}^{-}$, i.e. with (1i), $p=1$,

$$\boldsymbol{n}\times\boldsymbol{h}_1|_{\Gamma_{cpe,1}{}^{+}}=\boldsymbol{j}_{su,1}\ ,\quad \boldsymbol{n}\times\boldsymbol{h}_1|_{\Gamma_{cpe,1}{}^{-}}=0\ . \qquad (11a\text{-}b)$$

The perturbation problem $p=2$ then considers $\Omega_{cpe,2}=\Omega_{cpe,1}\subset\Omega_{c,2}$ with its finite conductivity σ_2, which alters the distribution of the eddy current density and the other fields. The fields in $\Omega_{cpe,2}$ are not surface fields anymore but penetrate the conductors. They are solutions of problem (1), $p=2$, with Ω_2 now comprising $\Omega_{cpe,2}$ but with particular ICs (1i-k) through $\Gamma_{cpe,2}=\partial\Omega_{cpe,2}$.

On the one hand, (1k), $p=2$, with (2) leads to

$$[\boldsymbol{n}\cdot\boldsymbol{b}_2]_{\Gamma_{cpe,2}}=\boldsymbol{b}_{su,2}=\boldsymbol{b}_{su}-\boldsymbol{b}_{su,1}=[\boldsymbol{n}\cdot\boldsymbol{b}]_{\Gamma_{cpe,2}}-\boldsymbol{b}_{su,1}=0, \qquad (12)$$

due to the continuity of $\boldsymbol{n}\cdot\boldsymbol{b}$ in the complete solution (2) and the zero value of $\boldsymbol{b}_{su,1}$ via (10a-b).

On the other hand, (1i), $p=2$, with (2) leads to

$$[\boldsymbol{n}\times\boldsymbol{h}_2]_{\Gamma_{cpe,2}}=\boldsymbol{j}_{su,2}=\boldsymbol{j}_{su}-\boldsymbol{j}_{su,1}=[\boldsymbol{n}\times\boldsymbol{h}]_{\Gamma_{cpe,2}}-\boldsymbol{j}_{su,1}=-\boldsymbol{n}\times\boldsymbol{h}_1|_{\Gamma_{cpe,1}{}^{+}}, \qquad (13)$$

due to the continuity of $\boldsymbol{n}\times\boldsymbol{h}$ in (2) and relation (11a).

The normal component of the perturbation magnetic flux density $\boldsymbol{b}_2$ is therefore continuous through $\Gamma_{cpe,2}$, whereas the tangential component of the perturbation magnetic field $\boldsymbol{h}_2$ is discontinuous and equals the opposite of the one of the reference field $\boldsymbol{h}_1$. This last trace field is a particularization of the volume source (5) for a surface perturbation.

IV. FINITE ELEMENT WEAK FORMULATIONS AND CONSTRAINTS

A. Reference formulation with surface currents

The eddy current problems p are defined in Ω_p with the magnetic vector potential formulation (Dular *et al.*, 2000),

expressing the electric field $\boldsymbol{e}_p$ in $\Omega_{c,p}$ via a magnetic vector potential $\boldsymbol{a}_p$ together with the gradient of an electric scalar potential v_p, and the magnetic flux density $\boldsymbol{b}_p$ in Ω_p as the curl of $\boldsymbol{a}_p$.

The resulting $\boldsymbol{a}$-v magnetodynamic formulation of problem $p=1$ is obtained from the weak form of the Ampère equation (1a), i.e. (Dular *et al.*, 2000),

$$(\mu_1^{-1}\operatorname{curl}\boldsymbol{a}_1,\operatorname{curl}\boldsymbol{a}')_{\Omega_1}+(\sigma_1\,\partial_t\boldsymbol{a}_1,\boldsymbol{a}')_{\Omega_{c,1}}+(\sigma_1\operatorname{grad}v_1,\boldsymbol{a}')_{\Omega_{c,1}}$$
$$+<\boldsymbol{n}\times\boldsymbol{h}_1,\boldsymbol{a}'>_{\Gamma_{h,1}}+<\boldsymbol{n}\times\boldsymbol{h}_1,\boldsymbol{a}'>_{\Gamma_{b,1}}=0\,,\ \forall\,\boldsymbol{a}'\in F_1{}^1(\Omega_1)\,, \quad (14)$$

where $F_1{}^1(\Omega_1)$ is a gauged curl-conform function space defined on Ω_1 and containing the basis functions for $\boldsymbol{a}$ as well as for the test function $\boldsymbol{a}'$ (at the discrete level, this space is defined by edge finite elements); $(\cdot,\cdot)_\Omega$ and $<\cdot,\cdot>_\Gamma$ respectively denote a volume integral in Ω and a surface integral on Γ of the product of their vector field arguments.

The surface integral term on $\Gamma_{h,1}$ accounts for natural BCs of type (1f). The term on the surface $\Gamma_{b,1}$ with essential BCs on $\boldsymbol{n}\cdot\boldsymbol{b}_1$ is usually omitted because it does not contribute locally to (14). It is however the key for expressing global currents (demonstrated hereafter) and post-processing the reference solution, a part of which being $\boldsymbol{n}\times\boldsymbol{h}_1|_{\Gamma_{b,1}}$ (this will be detailed in the next subsection).

The BC (10a) on each boundary $\Gamma_{cpe,1}$ leads to an essential BC on the primary unknown $\boldsymbol{a}_1$ that can be expressed via the definition of a surface scalar potential u_1 (in general single valued, if no net magnetic flux flows in $\Omega_{cpe,1}$) (Dular *et al.*, 2005), i.e.,

$$\boldsymbol{n}\cdot\operatorname{curl}\boldsymbol{a}_1\big|_{\Gamma_{cpe,1}}=0\Leftrightarrow\boldsymbol{n}\times\boldsymbol{a}_1\big|_{\Gamma_{cpe,1}}=\boldsymbol{n}\times\operatorname{grad}u_1\big|_{\Gamma_{cpe,1}}\,. \quad (15)$$

In a 2D model with currents in the third direction, condition (15) amounts to defining an unknown constant value for the perpendicular component of $\boldsymbol{a}_1$ for each conductor.

In the reference formulation (14), the perfect conductors are extracted from Ω_1 and $\Omega_{c,1}$ and are only involved through their boundaries $\Gamma_{cpe,1}$ with condition (15). This latter condition is to be strongly defined in $F_1{}^1(\Omega_1)$. The boundaries $\Gamma_{cpe,1}$ are thus to be added to $\Gamma_{b,1}$.

The surface integral term $<\boldsymbol{n}\times\boldsymbol{h}_1,\boldsymbol{a}'>_{\Gamma_{cpe,1}}$ is non-zero only for the function grad u' (from (15)), the value of which is then the total surface current I_1 flowing in $\Gamma_{cpe,1}$ (this can be demonstrated from the general procedure developed in (Dular *et al.*, 2005)). It is zero for all the other local test functions (at the discrete level, for any edge not belonging to $\Gamma_{cpe,1}$). This way, the circuit relation can be expressed for each conductor $\Omega_{cpe,1}$ and the coupling with electrical circuits is possible.

B. Perturbation formulation with surface sources

The weak magnetic vector potential formulation of the perturbation problem $p=2$ is

$$(\mu_2^{-1}\operatorname{curl}\boldsymbol{a}_2,\operatorname{curl}\boldsymbol{a}')_{\Omega_2}$$
$$+(\sigma_2\,\partial_t\boldsymbol{a}_2,\boldsymbol{a}')_{\Omega_{c,2}\setminus\Omega_{cpe,2}}+(\sigma_2\operatorname{grad}v_2,\boldsymbol{a}')_{\Omega_{c,2}\setminus\Omega_{cpe,2}}$$
$$+(\sigma_2\,\partial_t\boldsymbol{a}_2,\boldsymbol{a}')_{\Omega_{cpe,2}}+(\sigma_2\operatorname{grad}v_2,\boldsymbol{a}')_{\Omega_{cpe,2}}+<\boldsymbol{n}\times\boldsymbol{h}_2,\boldsymbol{a}'>_{\Gamma_{h,2}}$$
$$+<[\boldsymbol{n}\times\boldsymbol{h}_2]_{\Gamma_{cpe,2}},\boldsymbol{a}'>_{\Gamma_{cpe,2}}=0,\ \forall\,\boldsymbol{a}'\in F_2{}^1(\Omega_2)\,. \quad (16)$$

The approximation (6b) amounts to neglecting the second and third terms of (16), while (6a) acts on its first term.

A consequence of the $\boldsymbol{b}$-conform formulation is that ICs (12) and (13) are to be defined respectively in strong and weak senses. The IC (12) is strongly expressed in $F_2{}^1(\Omega_2)$ via the continuity of the tangential component of $\boldsymbol{a}_2$ through $\Gamma_{cpe,2}$. The IC (13) can rather only act in a weak sense via the surface integral term related to $\Gamma_{cpe,2}$ in (16). Indeed, the trace $\boldsymbol{n}\times\boldsymbol{h}_1$ is not known in a strong sense on $\Gamma_{cpe,2}{}^+$, but rather in a weak sense. Accordingly, the local determination of $\boldsymbol{n}\times\boldsymbol{h}_1$ must be avoided. The integral in which it appears is directly calculated instead. This latter can be developed as

$$<[\boldsymbol{n}\times\boldsymbol{h}_2]_{\Gamma_{cpe,2}},\boldsymbol{a}'>_{\Gamma_{cpe,2}}=<-\boldsymbol{n}\times\boldsymbol{h}_1,\boldsymbol{a}'>_{\Gamma_{cpe,2}{}^+}$$
$$=<-\boldsymbol{n}\times\boldsymbol{h}_1,\boldsymbol{a}'>_{\Gamma_{cpe,1}{}^+}=-(\mu_1^{-1}\operatorname{curl}\boldsymbol{a}_1,\operatorname{curl}\boldsymbol{a}')_{\Omega_1\setminus\Omega_{cpe,1}} \quad (17)$$

in case no part of $\Omega_{c,1}\setminus\Omega_{cpe,1}$ is in contact with $\Omega_{cpe,1}$ (otherwise the second and third terms of (14) have to be considered as well). This way, the surface integral term related to $\Gamma_{cpe,2}{}^+$ in (16) is naturally calculated from a volume integral coming from the reference problem. At the discrete level, this volume integral is usefully limited to one single layer of FEs touching the boundary.

Because the reference quantity $\boldsymbol{a}_1$ in (17) is initially given in the mesh of the reference problem, it has afterwards to be expressed in the mesh of the perturbation problem for being used in (17). This can be done through a projection method (Geuzaine *et al.*, 1999) of its curl limited to the layer of finite elements touching $\Omega_{cpe,1}$.

V. Application

A copper inductor with a square section is considered in a first test problem. The gap with the return path is reduced to 1.4 times the square side size (s) to allow proximity effects. The copper conductivity is taken as constant ($\sigma_{Cu}=5.9\,10^7\ \Omega^{-1}\mathrm{m}^{-1}$), although it varies in thermal analyses. A 2D model with a vertical symmetry axis is considered for this inductor (Fig. 1). For a direct comparison with the IBC technique, a frequency domain analysis is performed. However, the subdomain perturbation technique can be directly applied to time domain analyses without any change.

Several working frequencies are considered to cover a range of skin depths (δ). An associated normalized variable is the skin depth to square size ratio (δ/s) for which the particular values 0.05, 0.1, 0.2 and 0.4 are considered. A low ratio fulfills the assumption required by the IBC technique for obtaining an accurate solution along flat conducting regions, whereas the solution in the vicinity of edges and corners suffers from inaccuracies as it will be shown.

The magnetic flux lines of the reference solution are shown in Fig. 1. This solution serves as a source for each perturbation problem with a given ratio δ/s. Each perturbation solution (Fig. 2) is to be added to the reference one to give the actual associated magnetic flux solution (Fig. 3). The current density distribution in the inductor is however directly given by the perturbation solution (Fig. 4).

For allowing a direct comparison of the absolute importance of each solution, the magnetic flux lines in Figs. 1, 2 and 3 define equal flux tubes. It can then be observed that a decrease of the frequency, i.e. an increase of δ/s, leads to a perturbation solution of growing importance compared to the reference solution. This can be verified via the relative importance of the magnetic energy of the perturbation solution compared to the one of the complete solution, as shown in Fig. 5.

The perfect conductor solution usually overestimates the

magnetic flux density in the vicinity of corners and edges. The correction given by the perturbation solution is clearly shown in Fig. 2 where flux loops occur around the corners. This is also pointed out for a particular ratio δ/s in Fig. 6 (opposite direction of the perturbation magnetic flux density compared to the reference flux density). In addition to calculating the actual solution in the inductor, the perturbation problem reduces the reference solution in the exterior region.

Fig. 7 shows the current density distribution along the inductor surface calculated for different ratios δ/s with the conventional FE method, the perturbation technique and the IBC technique. The first two solutions are in perfect agreement, whereas the IBC underestimates the current density up to a distance of about $3\,\delta$ from each corner. The resulting error on the current and Joule power densities is shown in Fig. 8. It significantly increases in the vicinity of the conductor corners, up to 45% for the Joule power density and 25% for the current density. This affects the accuracy of the total losses (Fig. 9). As for the developed perturbation technique, it successfully and accurately adapts its solution to any frequency (or δ).

A second test problem consists of a transverse flux system with two 3-turn copper inductors on both sides of a conductive nonmagnetic plate. Half of a cross section of this system defines the considered 2D model (Fig. 10).

The inner aperture of the inductor is 20 mm, each inductor cross section is 10 mm by 6 mm and the gap between two successive turns is 2 mm. The copper conductivity is still considered as constant. The plate thickness is 2 mm. Two electric conductivities are considered for the plate ($\sigma_{Plate} = 10^6\,\Omega^{-1}\mathrm{m}^{-1}$ and $5\,10^7\,\Omega^{-1}\mathrm{m}^{-1}$). The working frequency of the inductor current is chosen for having $\delta/s = 0.2$, with $s = 10$ mm, i.e. $f = 1073$ Hz.

For this problem, the perturbation technique is applied only on the inductor. The plate is considered in the classical way. It is verified that, here again, the same level of inaccuracy is obtained with the IBC technique (around 25% for the inductor Joule losses), while the perturbation technique (Fig. 10) gives very accurate results. An accurate calculation of the current density distribution in the inductor is important for calculating its accurate coupling with the plate. The high conductive plate is responsible for an inverse proximity effect in the inductor, bringing the main current closer to the plate, while the opposite occurs with the low conductive plate. For high and low conductive plates, a uniform inductor current density would respectively underestimate and overestimate the Joule losses in the plate of 10% and 22%, in addition to underevaluating the Joule losses in the inductor.

VI. Conclusions

The developed subdomain perturbation method offers a way to uncouple FE regions in eddy current frequency and time domain analyses, allowing the solution process to be lightened. The skin and proximity effects in inductors can be accurately determined in a wide frequency range, allowing precise Joule losses calculations.

Once calculated, the reference solution can be used in various subproblems. This allows efficient parameterized analyses on the power supply and the electric conductivity (e.g. via a temperature dependence) of the inductors in a wide range, i.e. on parameters affecting the skin depth.

References

Badics, Z., Matsumoto, Y., Aoki, K., Nakayasu, F., Uesaka, M. and Miya, K. (1997), "An effective 3-D finite element scheme for computing electromagnetic field distorsions due to defects in eddy-current nondestructive evaluation," *IEEE Trans. Magn.*, Vol. 33, No. 2, pp. 1012-1020.

Dular, P., Kuo-Peng, P., Geuzaine, C., Sadowski, N. and Bastos, J.P.A. (2000), "Dual magnetodynamic formulations and their source fields associated with massive and stranded inductors," *IEEE Trans. Magn.*, Vol. 36, No. 4, pp. 3078-3081.

Dular, P., Gyselinck, J., Henneron, T. and Piriou, F. (2005), "Dual finite element formulations for lumped reluctances coupling," *IEEE Trans. Magn.*, Vol. 41, No. 5, pp. 1396-1399.

Dular, P. and Sabariego, R. V. (2007), "A perturbation method for computing field distortions due to conductive regions with h-conform magnetodynamic finite element formulations," *IEEE Trans. Magn.*, Vol. 43, No. 4, pp. 1293-1296.

Dular, P., Sabariego, R. V., Gyselinck, J. and Krähenbühl, L. (2007), "Sub-domain finite element method for efficiently considering strong skin and proximity effects," *COMPEL*, Vol. 26, No. 4, pp. 974-985.

Geuzaine, C., Meys, B., Henrotte, F., Dular, P. and Legros, W. (1999), "A Galerkin projection method for mixed finite elements," *IEEE Trans. Magn.*, Vol. 35, No. 3, pp. 1438-1441.

Krähenbühl, L. and Muller, D. (1993), "Thin layers in electrical engineering. Example of shell models in analyzing eddy-currents by boundary and finite element methods," *IEEE Trans. Magn.*, Vol. 29, No. 2, pp. 1450-1455.

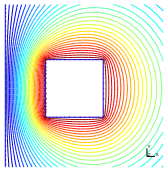

Fig. 1. Two-dimensional model (right part of the inductor and vertical symmetry axis on the left) and magnetic flux lines (phase 0) for the reference solution $\boldsymbol{b}_1$.

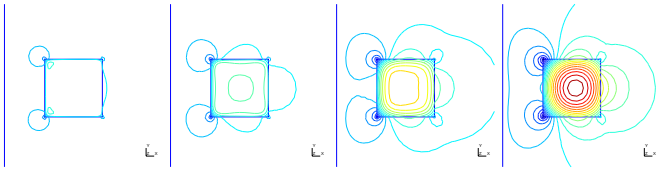

Fig. 2. Magnetic flux lines (phase 0) for the perturbation solution $\boldsymbol{b}_2$ (from *left* to *right* for δ/s = 0.05, 0.1, 0.2 and 0.4).

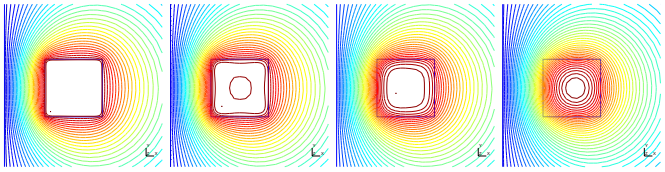

Fig. 3. Magnetic flux lines (phase 0) for the perturbed solution $\boldsymbol{b}$ (from *left* to *right* for δ/s = 0.05, 0.1, 0.2 and 0.4).

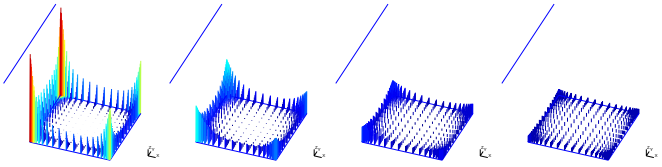

Fig. 4. Current density distribution (modulus) for the perturbation solution (from *left* to *right* for δ/s = 0.05, 0.1, 0.2 and 0.4).

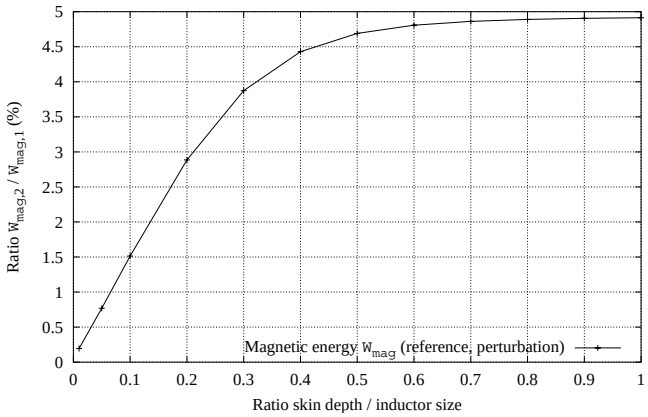

Fig. 5. Importance of the magnetic energy of the perturbation solution with respect to the reference solution as a function of the skin depth – inductor size ratio.

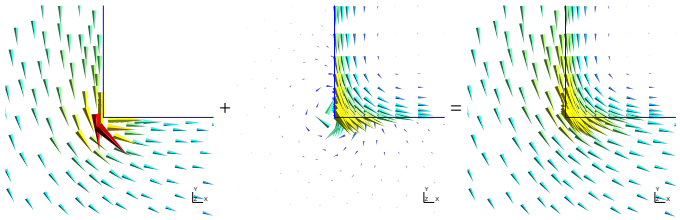

Fig. 6. Magnetic flux density (zoom on the lower left corner of the inductor; phase 0; for $\delta/s = 0.1$) for the reference solution (*left*) and the perturbation solution (*middle*), the sum of which gives the complete solution (*right*).

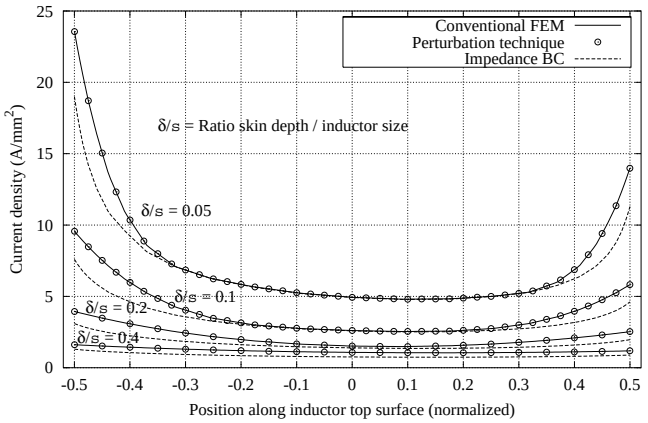

Fig. 7. Current density modulus along the inductor top surface for the conventional FE solution, the perturbation technique and the IBC technique; the position is normalized for varying from –0.5 to 0.5 along the square side, allowing a direct comparison with the ratio δ/s.

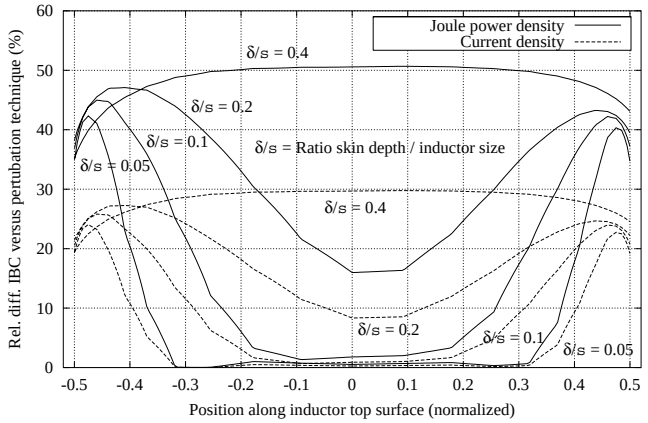

Fig. 8. Relative differences between the solutions (Joule power and current densities) of the perturbation and IBC techniques.

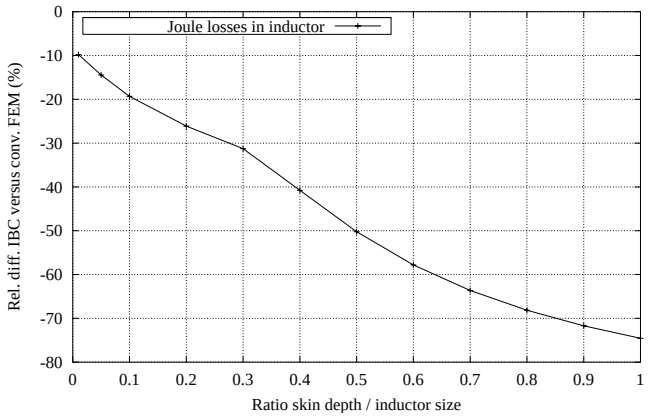

Fig. 9. Inaccuracy of the IBC technique for the Joule losses calculation in a conductor with corners as a function of the skin depth – inductor size ratio.

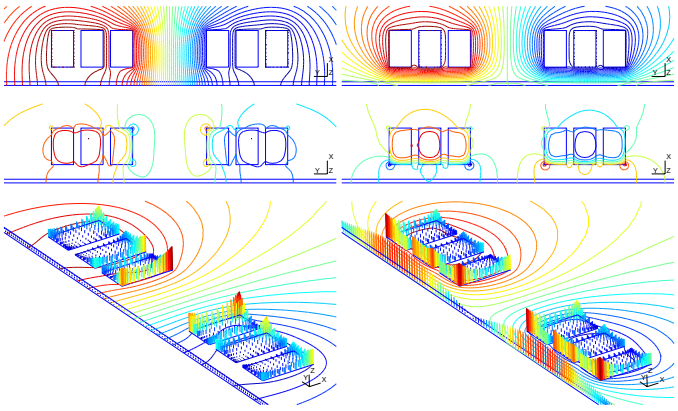

Fig. 10. Two-dimensional model of a transverse flux system (3-turn inductor above a half plate, with perpendicular flux horizontal symmetry axis below); a low (*left*) and a high (*right*) electric conductivity are considered for the plate; from *top* to *bottom*: magnetic flux lines (phase 0) for the reference solution $\boldsymbol{b}_1$ with a perfectly conductive inductor, the perturbation solution $\boldsymbol{b}_2$ and the perturbed solutions $\boldsymbol{b}$ (for $\delta/s = 0.2$, with s the height of the inductor); *bottom*: current density distribution (modulus).